

A computer-algebraic investigation of an oscillating boundary layer

KARL G. ROESNER

Darmstadt, Germany

<http://www.kgroesner.de>, e-mail: kgroesner@t-online.de

For large Reynolds numbers analytical expressions are derived for the velocity components and the pressure in the boundary layer between two oscillating parallel planes. The linearization of the boundary layer equations leads to a coupled system of three parabolic differential equations with time-dependent or homogeneous boundary conditions. The solutions are derived using computer algebra software on a personal computer. The vortical character of the flow pattern — shown in experiments — resembles the famous Görtler vortices in the boundary layer along a curved wall. A criterion for vortex identification for this type of motion is at least fulfilled for half the period of the oscillating planes.

Keywords: boundary layer, time-periodic flow, pattern formation, Görtler vortices, parabolic differential equations, vortex identification, computer algebra.

Introduction

The following investigation is based on a computer-algebraic analysis of the time-dependent boundary layer equations, describing the oscillating flow in a fluid layer between two parallel plates induced by the torsional motion of the boundaries. The analytical solution of the linearized boundary layer equations results from the solution of three parabolic differential equations describing the initial-boundary value problems for the velocity components. The solution which defines the velocity components can be split into three terms, describing the transient, oscillating and stationary flow in radial and axial direction. The stationary flow is responsible for the mass transport in the boundary layer. Experiments show a formation of streamwise vortices in the boundary layer. Once the cylinder is set into oscillation, in the vicinity of the axis of rotation — close to top and bottom boundary — vortices are created, which propagate radially outward. This phenomenon resembles the well known Görtler vortices along concave walls. In the present case, the curved streamlines in the stagnation region play the role of a concave rigid wall, which causes Görtler vortices along the curved boundary. In the present case the vortex character of the flow can be analysed using the symmetric and skew symmetric part of the vector gradient of the Navier — Stokes equations. It can be shown that a local pressure minimum exists due to vortical motion [1]. In Fig. 1 the vortical structure in the vicinity of the axis of an oscillating flat cylinder results from the self organisation of the fluid under the torsional motion around the axis. The initially separated radial vortices interact while being pulled outward radially under the action of the steady radial flow enforced by the centrifugal force. This leads at last to a pattern of entangling interacting vortices.

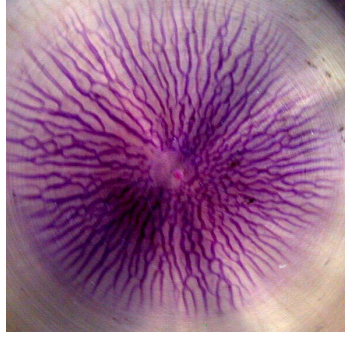


Fig. 1. Streamwise vortices in an oscillating boundary layer

1. Basic equations and boundary conditions

In a cylindrical coordinate system (r, φ, z) , the Navier — Stokes equations in the following form describe the cylindrical flow of a fluid with circumferential symmetry character. This means that the functions u, v, w, p and all their partial derivatives with respect to φ are not depending on the independent variable φ .

$$\frac{\partial u}{\partial t} + u \frac{\partial u}{\partial r} + w \frac{\partial u}{\partial z} - \frac{v^2}{r} = -\frac{1}{\rho} \frac{\partial p}{\partial r} + \nu \left[\frac{\partial^2 u}{\partial r^2} + \frac{1}{r} \frac{\partial u}{\partial r} - \frac{u}{r^2} + \frac{\partial^2 u}{\partial z^2} \right], \quad (1)$$

$$\frac{\partial v}{\partial t} + u \frac{\partial v}{\partial r} + w \frac{\partial v}{\partial z} + \frac{uv}{r} = \nu \left[\frac{\partial^2 v}{\partial r^2} + \frac{1}{r} \frac{\partial v}{\partial r} - \frac{v}{r^2} + \frac{\partial^2 v}{\partial z^2} \right], \quad (2)$$

$$\frac{\partial w}{\partial t} + u \frac{\partial w}{\partial r} + w \frac{\partial w}{\partial z} = -\frac{1}{\rho} \frac{\partial p}{\partial z} + \nu \left[\frac{\partial^2 w}{\partial r^2} + \frac{1}{r} \frac{\partial w}{\partial r} + \frac{\partial^2 w}{\partial z^2} \right]. \quad (3)$$

u, v, w are the velocity components in r -, φ - and z -direction, p is the pressure and ν is the kinematic viscosity of the fluid. In addition, the continuity equation reads like

$$\frac{1}{r} \frac{\partial(ru)}{\partial r} + \frac{\partial w}{\partial z} = 0. \quad (4)$$

We assume that the motion of the two parallel planes, oscillating with the frequency n around the common axis, is limited to small angular amplitudes $\omega \ll 1$, that the following estimation holds:

$$\Omega(t) = \omega \sin nt \ll 1.$$

The circumferential velocity component of boundary points in the planes $z = 0$ and $z = d$, is therefore prescribed by the function

$$v(r, 0, t) = v(r, d, t) = r \Omega_0 \cos nt, \quad \Omega_0 := \omega n,$$

where d is the vertical distance of the parallel plates. This boundary condition prescribes a harmonic oscillation of the two planes parallel to each other with the frequency n and the velocity amplitude $r\Omega_0$ around the z -axis.

For the radial and axial velocity components $u(r, z, t)$ and $w(z, t)$ we get homogeneous boundary conditions at $z = 0$ and $z = d$:

$$\begin{aligned} u(r, 0, t) &= u(r, d, t) = 0, \\ w(0, t) &= w(d, t) = 0. \end{aligned}$$

2. Nondimensional equations

The variables $u(r, z, t)$, $v(r, z, t)$, $w(z, t)$ and $p(z, r, t)$ are transformed into dimensionless form introducing the distance d of the two planes as length scale for the coordinates z and r and the frequency n for the time t .

$$\bar{y} := \frac{z}{d}, \quad \bar{r} := \frac{r}{d}, \quad \bar{t} := nt.$$

The nondimensional velocity components and the pressure are defined as follows:

$$\bar{u} := \frac{u(r, z, t)}{\Omega_0 d}, \quad \bar{v} := \frac{v(r, z, t)}{\Omega_0 d}, \quad \bar{w} := \frac{w(z, t)}{\Omega_0 d}, \quad \bar{p} := \frac{p(r, z, t)}{\rho \Omega_0^2 d^2}.$$

Introducing the parameter

$$\omega := \frac{\Omega_0}{n},$$

which represents the ratio of the amplitude of the angular velocity and the frequency of oscillation of the planes, into the dimensionless system of differential equations leads to the following system of equations:

$$\frac{1}{\omega} \frac{\partial \bar{u}}{\partial \bar{t}} + \bar{u} \frac{\partial \bar{u}}{\partial \bar{r}} + \bar{w} \frac{\partial \bar{u}}{\partial \bar{y}} - \frac{\bar{v}^2}{\bar{r}} = -\frac{\partial \bar{p}}{\partial \bar{r}} + \frac{\nu}{d^2 \Omega_0} \left[\frac{\partial^2 \bar{u}}{\partial \bar{r}^2} + \frac{1}{\bar{r}} \frac{\partial \bar{u}}{\partial \bar{r}} - \frac{\bar{u}}{\bar{r}^2} + \frac{\partial^2 \bar{u}}{\partial \bar{y}^2} \right], \quad (5)$$

$$\frac{1}{\omega} \frac{\partial \bar{v}}{\partial \bar{t}} + \bar{u} \frac{\partial \bar{v}}{\partial \bar{r}} + \bar{w} \frac{\partial \bar{v}}{\partial \bar{y}} + \frac{\bar{u} \bar{v}}{\bar{r}} = \frac{\nu}{d^2 \Omega_0} \left[\frac{\partial^2 \bar{v}}{\partial \bar{r}^2} + \frac{1}{\bar{r}} \frac{\partial \bar{v}}{\partial \bar{r}} - \frac{\bar{v}}{\bar{r}^2} + \frac{\partial^2 \bar{v}}{\partial \bar{y}^2} \right], \quad (6)$$

$$\frac{1}{\omega} \frac{\partial \bar{w}}{\partial \bar{t}} + \bar{u} \frac{\partial \bar{w}}{\partial \bar{r}} + \bar{w} \frac{\partial \bar{w}}{\partial \bar{y}} = -\frac{\partial \bar{p}}{\partial \bar{y}} + \frac{\nu}{d^2 \Omega_0} \left[\frac{\partial^2 \bar{w}}{\partial \bar{r}^2} + \frac{1}{\bar{r}} \frac{\partial \bar{w}}{\partial \bar{r}} + \frac{\partial^2 \bar{w}}{\partial \bar{y}^2} \right], \quad (7)$$

$$\frac{1}{\bar{r}} \frac{\partial(\bar{r} \bar{u})}{\partial \bar{r}} + \frac{\partial \bar{w}}{\partial \bar{y}} = 0. \quad (8)$$

The dimensionless boundary conditions are

$$\begin{aligned} \bar{u}(\bar{r}, 0, \bar{t}) &= \bar{u}(\bar{r}, 1, \bar{t}) = 0, \\ \bar{v}(\bar{r}, 0, \bar{t}) &= \bar{v}(\bar{r}, 1, \bar{t}) = \bar{r} \cos \bar{t}, \\ \bar{w}(0, \bar{t}) &= \bar{w}(1, \bar{t}) = 0. \end{aligned}$$

3. The ansatz functions

Introducing the ansatz functions [2], [3], $F(\bar{y}, \bar{t})$, $g(\bar{y})$, and $P(\bar{y}, \bar{t})$, the velocity components \bar{u} , \bar{v} , \bar{w} and \bar{p} are defined in the following way:

$$\begin{aligned} \bar{u}(\bar{r}, \bar{y}, \bar{t}) &= \bar{r} \omega F_{\bar{y}}(\bar{y}, \bar{t}), \\ \bar{v}(\bar{r}, \bar{y}, \bar{t}) &= \bar{r} g(\bar{y}, \bar{t}), \\ \bar{w}(\bar{y}, \bar{t}) &= -2\omega F(\bar{y}, \bar{t}), \\ \bar{p}(\bar{r}, \bar{y}, \bar{t}) &= P(\bar{y}, \bar{t}) + \frac{1}{2} \bar{r}^2 K(\bar{t}). \end{aligned}$$

This choice of ansatz functions is similar to the analytical approach of the flow near a rotating disk which was analysed the first time by Th. v. Kármán.

The functions \bar{u}, \bar{v} depend linearly on \bar{r} . \bar{w} is independent of \bar{r} according to the fact, that the boundary layer thickness δ of the flow around the stagnation point at the plate is constant, not depending on the radius \bar{r} . \bar{p} contains the so-called centrifugal term, modified by the factor $K(\bar{t})$, which takes into account the time dependent influence of the centrifugal force. Introducing the ansatz functions into the system (5)–(8) — omitting the bar on the dimensionless quantities and denoting the dimensionless time by τ , we arrive at the following system of partial differential equations for the fluid under consideration with the Reynolds number

$$R := \frac{nd^2}{\nu} > 0, \quad (9)$$

$$F_{y\tau} + \omega^2 [F_y^2 - 2FF_{yy}] - g^2 = -K(\tau) + \frac{1}{R}F_{yyy}, \quad (10)$$

$$g_\tau + 2\omega^2 [F_y g - Fg_y] = \frac{1}{R}g_{yy}, \quad (11)$$

$$F_\tau - 2\omega^2 FF_y = \frac{1}{2}P_y + \frac{1}{R}F_{yy}. \quad (12)$$

The boundary conditions for the ansatz functions are

$$\begin{aligned} F(0, \tau) &= F(1, \tau) = 0, \\ F_y(0, \tau) &= F_y(1, \tau) = 0, \\ g(0, \tau) &= g(1, \tau) = \cos \tau. \end{aligned}$$

The ansatz functions fulfill the continuity equation identically. In addition to these boundary conditions the functions have to show the following symmetry and antisymmetry character, respectively:

$$\begin{aligned} F_y(y, \tau) &= F_y(1 - y, \tau), \\ F(y, \tau) &= -F(1 - y, \tau), \\ g(y, \tau) &= g(1 - y, \tau), \\ P(y, \tau) &= P(1 - y, \tau). \end{aligned}$$

4. The boundary layer approximation

Based on the assumption that Ω_0 is of order $0.1 \text{ s}^{-1} = 5.7^\circ \text{ s}^{-1}$, we assume

$$\omega^2 \ll 1, \quad (13)$$

which can be realised experimentally for a moderate n of about 50 s^{-1} . As a consequence of this assumption the differential equations are linearized and define the boundary layer equations for the flow in the vicinity of a fast oscillating plane:

$$F_{y\tau} = \frac{1}{R}F_{yyy} + g^2(y, \tau) - K(\tau), \quad (14)$$

$$g_\tau = \frac{1}{R}g_{yy}, \quad (15)$$

$$F_\tau = \frac{1}{R}F_{yy} + \frac{1}{2}P_y. \quad (16)$$

These equations can be solved analytically. In (14) we introduce a new function

$$\Phi(y, \tau) := F_y(y, \tau) \quad (17)$$

and get an inhomogeneous parabolic differential equation with homogeneous boundary conditions of the form

$$\Phi_\tau = \frac{1}{R}\Phi_{yy} + g^2(y, \tau) - K(\tau). \quad (18)$$

The solution of this equation determines the radial component

$$u(r, y, \tau) = r\omega \Phi(y, \tau).$$

Integrating equation (14) with respect to y , we get

$$F_\tau = \frac{1}{R}F_{yy} + \int g^2(y, \tau) dy - yK(\tau) + C_0(\tau), \quad (19)$$

the solution of this equation determines the axial velocity component

$$w(y, \tau) = -2\omega F(y, \tau).$$

If we compare (16) with (19), the pressure function $P(y, \tau)$ can be found by a twofold quadrature:

$$P(y, \tau) = 2 \int^y \left(\int^\eta g^2(\zeta, \tau) d\zeta \right) d\eta - y^2 K(\tau) + yC_0(\tau) + C_1(\tau). \quad (20)$$

As only the pressure gradient is physically relevant, we can assume $C_1(\tau) \equiv 0$.

The three parabolic differential equations for the velocity components and the relation for the pressure function are solved successively in the following order:

$$\begin{aligned} g_\tau &= \frac{1}{R}g_{yy}, \\ P(y, \tau) &= 2 \int^y \left(\int^\eta g^2(\zeta, \tau) d\zeta \right) d\eta - y^2 K(\tau) + yC_0(\tau), \\ \Phi_\tau &= \frac{1}{R}\Phi_{yy} + g^2(y, \tau) - K(\tau), \\ F_\tau &= \frac{1}{R}F_{yy} + \int g^2(y, \tau) dy - yK(\tau). \end{aligned}$$

5. The circumferential velocity component

A solution of (15) which obeys the time dependent boundary conditions is defined by

$$g(y, \tau) := G_1(y) \cos \tau - G_2(y) \sin \tau, \quad (21)$$

$$\begin{aligned} G_1(y) &: = e^{\lambda y} (\gamma_{11} \cos \lambda y - \gamma_{12} \sin \lambda y) + e^{-\lambda y} (\gamma_{21} \cos \lambda y + \gamma_{22} \sin \lambda y), \\ G_2(y) &: = e^{\lambda y} (\gamma_{12} \cos \lambda y + \gamma_{11} \sin \lambda y) + e^{-\lambda y} (\gamma_{22} \cos \lambda y - \gamma_{21} \sin \lambda y). \end{aligned}$$

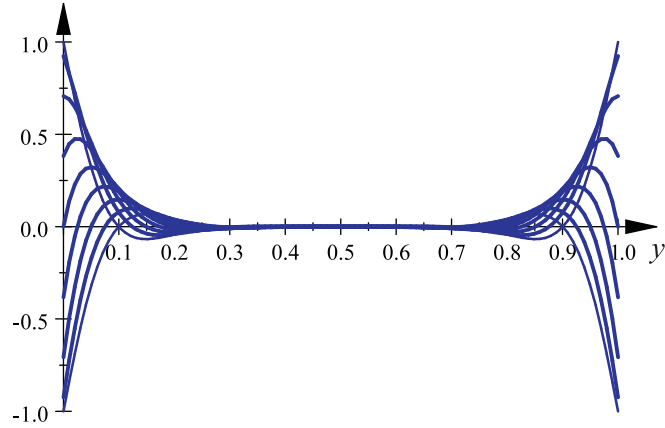


Fig. 2. $\frac{v(r, y, \tau)}{r\omega}$, $\tau = k\frac{\pi}{8}$, $k = 0, \dots, 8$

The coefficients γ_{ik} , $i, k = 1, 2$ are summarized in Appendix I. As initial condition we define $g(y, 0) := G_1(y)$.

Writing (21) in a slightly different form we get

$$g(y, \tau) = e^{y\lambda} (\gamma_{11} \cos(y\lambda - \tau) - \gamma_{12} (\sin(y\lambda + \tau))) + e^{-y\lambda} (\gamma_{21} \cos(y\lambda + \tau) + \gamma_{22} \sin(y\lambda - \tau)).$$

This can be interpreted as a superposition of two damped waves running from each of the boundaries into the interior of the fluid layer with the phase velocity

$$v_{phase} = \pm \frac{1}{\lambda} = \pm \sqrt{\frac{2}{R}}.$$

The circumferential velocity distribution in the fluid layer is therefore

$$v(r, y, \tau) = r\omega (G_1(y) \cos \tau - G_2(y) \sin \tau). \quad (22)$$

Figure 2 shows a sequence of velocity distributions in the fluid layer for nine time steps. For a chosen Reynolds number of $R = 500$, the oscillating walls influence a fluid layer of approximately 20% of the total thickness of the fluid.

Taking into account the initial condition for $g(y, \tau)$, we have to add the transient part to the solution (21). The transient solution of the homogeneous differential equation is given by

$$g_h^{tr} = \sum_{n=1}^{\infty} A_n e^{-\frac{\pi^2 n^2}{R} \tau} \sin n\pi y.$$

The coefficients A_n are listed in the Appendix II. After a transient time of $\tau = 20$ the maximal amplitude of g_h^{tr} is approximately of order 10^{-4} . Therefore, for further calculations only the time periodic solution (22) will be used.

6. The pressure function

Performing the twofold quadrature in (20) results in the following solution

$$P(y, \tau) = 2 (\Pi_1(y) \cos^2 \tau + \Pi_2(y) \sin^2 \tau - \Pi_3(y) \sin 2\tau) - y^2 K(\tau) + yC_0(\tau).$$

The functions Π_1, Π_2, Π_3 are listed explicitly in the Appendix III. From the symmetry character of $P(y, \tau)$ one derives the two expressions for $K(\tau)$ and $C_0(\tau)$

$$K(\tau) = (\gamma_{11}\gamma_{21} - \gamma_{12}\gamma_{22}) \cos 2\tau, \quad (23)$$

$$C_0(\tau) = 2(\gamma_{11}\gamma_{22} + \gamma_{12}\gamma_{21}) \sin 2\tau. \quad (24)$$

Finally, the pressure function $P(y, \tau)$ is given by

$$P(y, \tau) = 2(\Pi_1(y) \cos^2 \tau + \Pi_2(y) \sin^2 \tau - \Pi_3(y) \sin 2\tau) - y^2(\gamma_{11}\gamma_{21} - \gamma_{12}\gamma_{22}) \cos 2\tau + 2y(\gamma_{11}\gamma_{22} + \gamma_{12}\gamma_{21}) \sin 2\tau. \quad (25)$$

7. The radial velocity component

Equation (18) is an inhomogeneous parabolic differential equation with homogeneous boundary conditions and the initial condition $\Phi(y, 0) = 0$. The solution of this initial-boundary value problem is represented by an expansion with respect to the eigenfunctions $\sin(n\pi y)$, $n \in \mathbb{N}$, of the homogeneous equation. In a first step the inhomogeneity has to be developed into a series of the eigenfunctions which leads to coefficients $U(k), V(k), W(k)$, which are listed in the Appendix IV.

$$\begin{aligned} g^2(y, \tau) - K(\tau) &= \\ &= 2 \sum_{k=0}^{\infty} (U(k) \cos^2 \tau + V(k) \sin^2 \tau - W(k) \sin 2\tau) \sin(2k+1)\pi y + \\ &\quad + 2(\gamma_{11}\gamma_{21} - \gamma_{12}\gamma_{22}) \sum_{k=0}^{\infty} \frac{R\kappa}{4R^2 + \kappa^2} e^{-\frac{\kappa}{R}\tau} \sin(\pi(2k+1)y) - \\ &\quad - 2(\gamma_{11}\gamma_{21} - \gamma_{12}\gamma_{22}) \sum_{k=0}^{\infty} R \frac{2R \sin 2\tau + \kappa \cos 2\tau}{4R^2 + \kappa^2} \sin(\pi(2k+1)y). \end{aligned} \quad (26)$$

As mentioned at the beginning, the solution of equation (18) can be split into three separate parts which will be denoted by the abbreviations: *tr* for transient, *os* for oscillation, and *st* for stationary flow. The indices *i* and *h* stand for inhomogeneous or homogeneous, respectively.

The transient solution

$$\begin{aligned} \frac{1}{r\omega} u(y, \tau)_i^{tr} &= \\ &= 2 \sum_{k=0}^{\infty} \left(\frac{-RU(k)(2R^2 + \kappa^2) - 2V(k)R^3 + W(k)R\kappa^2}{\kappa(\kappa^2 + 4R^2)} + \right. \\ &\quad \left. + \gamma \frac{R\kappa(1 - \cos \pi(2k+1))}{(4R^2 + \kappa^2)(2k+1)\pi} \right) e^{-\frac{\kappa}{R}\tau} \sin(2k+1)\pi y, \end{aligned} \quad (27)$$

$$\gamma : = \gamma_{11}\gamma_{21} - \gamma_{12}\gamma_{22},$$

$$\kappa : = \pi^2(2k+1)^2.$$

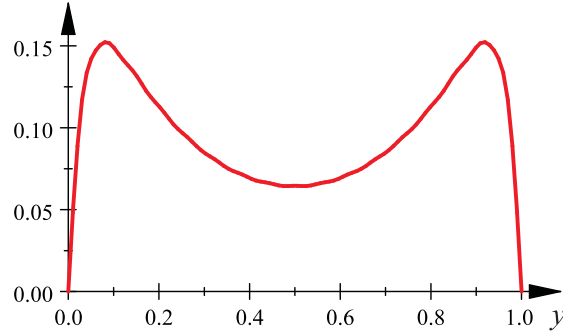


Fig. 3. $\frac{u_i^{st}(r, y, \tau)}{r\omega}$ radial component

The oscillating solution

$$\begin{aligned} & \frac{1}{r\omega} u(y, \tau)_i^{os} = \\ & = \sum_{k=0}^{\infty} \left(\frac{R}{\kappa^2 + 4R^2} \begin{pmatrix} U(k)\kappa \cos 2\tau + 2R \sin 2\tau - \\ -V(k)(\kappa \cos 2\tau + 2R \sin 2\tau - \kappa) - \\ -2W(k)\kappa \cos 2\tau + 2R \sin 2\tau \\ -2\gamma R \frac{(2R \sin 2\tau + \kappa \cos 2\tau)(1 - \cos \pi(2k+1))}{(4R^2 + \kappa^2)(2k+1)\pi} \end{pmatrix} \right) \sin(2k+1)\pi y. \end{aligned} \quad (28)$$

The stationary solution

$$u(y, \tau)_i^{st} = \sum_{k=0}^{\infty} \frac{R(U(k) + V(k)) - 2}{\kappa} \sin(\pi(2k+1)y). \quad (29)$$

As (29) is a fast convergent series, it is sufficient to take into account only 20 terms. The approximate solution

$$\sum_{k=0}^{20} \frac{R(U(k) + V(k)) - 2}{\kappa} \sin(\pi(2k+1)y)$$

is shown in Fig. 3, where $R = 500$.

This velocity profile indicates the boundary layer character of the flow by a strong velocity gradient close to the walls.

The stationary flow in radial direction is responsible for the formation of streamwise vortices within the boundary layer. The transient part of the solution decays very fast, and the oscillating behavior is not responsible for the radial material transport, which is observed in the experiment. Therefore only the stationary term plays the major role in the analysis of the vortex formation.

8. The axial velocity component

The component $w(y, \tau)$ can be calculated by solving the partial differential equation (19)

$$F_\tau = \frac{1}{R} F_{yy} + \int g^2(y, \tau) dy - yK(\tau) + C_0(\tau)$$

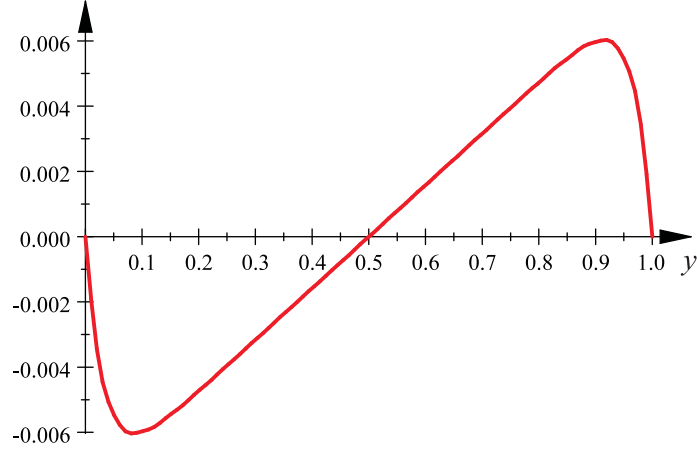


Fig. 4. $-\frac{w_i^{st}(y, \tau)}{\omega}$ axial component

with given functions $K(\tau)$ and $C_0(\tau)$, defined by formulas (23), (24). The inhomogeneity

$$\int g^2(y, \tau) dy - yK(\tau) + C_0(\tau)$$

must be developed into a series with respect to the eigenfunctions $\sin(n\pi y)$ and contributes to the solution as a driving term. The complete solution is a superposition of the three parts:

The transient solution

$$\begin{aligned} &-\frac{1}{\omega}w_i^{tr}(y, \tau) = \\ &= 2 \sum_{k=1}^{\infty} \left(\frac{\Theta_1 R (2R^2 + \pi^4 n^4) + 2\Theta_2 R^3 + 2\Theta_3 R^2 \pi^2 n^2}{\pi^2 (2k)^2 (\pi^4 (2k)^4 + 4R^2)} - \frac{(\gamma \pi^2 (2k)^2 + 8\Gamma_2 R) R \cos 2k\pi}{4k\pi (4R^2 + \pi^4 (2k)^4)} \right) e^{-\frac{\pi^2}{R}(2k)^2 \tau} \sin 2k\pi y. \end{aligned} \quad (30)$$

The oscillating solution

$$\begin{aligned} &\Gamma_2 := (\gamma_{11}\gamma_{22} - \gamma_{12}\gamma_{21}), \\ &-\frac{1}{\omega}w_i^{os}(y, \tau) = 2 \sum_{k=1}^{\infty} \left((\Theta_1 - \Theta_2) \frac{R (\pi^2 (2k)^2 \cos 2\tau + 2R \sin 2\tau)}{2 (\pi^4 (2k)^4 + 4R^2)} + \Theta_3 R \frac{2R \cos 2\tau + \pi^2 (2k)^2 \sin 2\tau}{4R^2 + \pi^4 (2k)^4} + \Theta_4 \right) \sin 2k\pi y. \end{aligned} \quad (31)$$

The stationary solution

$$-\frac{1}{\omega}w_i^{st} = \sum_{k=1}^{\infty} \left(R \frac{\Theta_1 + \Theta_2}{\pi^2 (2k)^2} + \frac{2RK(\tau)}{\pi^3 (2k)^3} \cos 2k\pi \right) \sin (2k\pi y). \quad (32)$$

The coefficients $\Theta_1, \Theta_2, \Theta_3$ are summarized in the Appendix V. For the Reynolds number $R = 500$ the graph of the axial velocity component is given in Fig. 4.

9. Vortex identification

From several existing criteria, how to define a vortex in the flow field, the one which was stated by the authors Jeong and Hussain is the most convincing one and was used in the present investigation. By a decomposition of the vector gradient of the Navier—Stokes equations into a symmetric part S and a skew symmetric part A , the eigenvalues μ_1, μ_2, μ_3 of the symmetric matrix

$$S^2 + A^2 = \begin{pmatrix} \omega^2 F_y^2 - g^2 & 0 & -\frac{r(F_y F_{yy} \omega^2 + g g_y)}{2} \\ 0 & \omega^2 F_y^2 - g^2 & \frac{r\omega(g F_{yy} - F_y g_y)}{2} \\ -\frac{r(F_y F_{yy} \omega^2 + g g_y)}{2} & \frac{r\omega(g F_{yy} - F_y g_y)}{2} & 4\omega^2 F_y^2 \end{pmatrix} \quad (33)$$

are calculated:

$$\mu_1(y, \tau) = -\frac{g^2}{2} + \frac{5\omega^2 F_y^2}{2} + \frac{1}{2} \sqrt{\begin{matrix} g^2(g^2 + r^2 g_y^2) + \\ +\omega^2 \left(g^2(r^2 F_{yy}^2 + 6F_y^2) + \right. \\ \left. + r^2 F_y^2 g_y^2 \right) \\ \left. + \omega^4 F_y^2 (r^2 F_{yy}^2 + 9F_y^2) \right)} + , \quad (34)$$

$$\mu_2(y, \tau) = -\frac{g^2}{2} + \frac{5\omega^2 F_y^2}{2} - \frac{1}{2} \sqrt{\begin{matrix} g^2(g^2 + r^2 g_y^2) + \\ +\omega^2 \left(g^2(r^2 F_{yy}^2 + 6F_y^2) + \right. \\ \left. + r^2 F_y^2 g_y^2 \right) \\ \left. + \omega^4 F_y^2 (r^2 F_{yy}^2 + 9F_y^2) \right)} + , \quad (35)$$

$$\mu_3(y, \tau) = \omega^2 F_y^2 - g^2. \quad (36)$$

According to $\omega^2 \ll 1$ we can neglect all terms of order ω^2 and higher. Therefore we get

$$\mu_1(y, \tau) \approx -\frac{1}{2}g^2 + \frac{1}{2}g\sqrt{g^2 + r^2 g_y^2} > 0, \quad (37)$$

$$\mu_2(y, \tau) \approx -\frac{1}{2}g^2 - \frac{1}{2}g\sqrt{g^2 + r^2 g_y^2} < 0, \quad (38)$$

$$\mu_3(y, \tau) \approx -g^2 < 0, \quad 0 \leq \tau \leq \pi/2. \quad (39)$$

Summing up the three eigenvalues we find

$$\sum_{i=1}^3 \mu_i(y, \tau) < 0$$

which fulfills together with (37)–(39) the criterion for the existence of vortical structures in the flow field. The strong velocity gradient in the shear layer close to the oscillating plates is the region where vortices can be created and grow.

Acknowledgement

The manuscript was written using the software Scientific Workplace, Version 5.5, and most of the algebraic calculations were performed by the built-in MAPLE software.

References

- [1] **Jeong, J. and Hussain, F.** On the identification of a vortex // J. Fluid Mech. 1995. Vol. 285. P. 69–94.
- [2] **v. Kármán, Th.** Laminare und turbulente Reibung // ZAMM. 1921. Vol. 1. P. 233–252.
- [3] **Rosenblat, S.** Flow between torsionally oscillating disks // J. Fluid Mech. 1960. Vol. 8. P. 388–399.

Appendix I

$$\lambda := \sqrt{\frac{R}{2}},$$

$$\gamma_{11} : = \frac{m_0 (e^{-2\lambda} - \cos 2\lambda) + 2m_1 \sinh \lambda \cos \lambda}{2 (\cosh 2\lambda - \cos 2\lambda)},$$

$$\gamma_{12} : = \frac{m_0 \cos \lambda \sin \lambda - m_1 \cosh \lambda \sin \lambda}{\cosh 2\lambda - \cos 2\lambda},$$

$$\gamma_{21} : = \frac{m_0 (e^{2\lambda} - \cos 2\lambda) - 2m_1 \sinh \lambda \cos \lambda}{4 (\sinh^2 \lambda + \sin^2 \lambda)},$$

$$\gamma_{22} : = \frac{m_1 \cosh \lambda \sin \lambda - m_0 \cos \lambda \sin \lambda}{2 (\sinh^2 \lambda + \sin^2 \lambda)},$$

$$m_0 = 1 \text{ and } m_1 = 1 : \text{co-oscillation,}$$

$$m_0 = 1 \text{ and } m_1 = -1 : \text{counter-oscillation.}$$

Appendix II

$$A_n = 2 \left(\begin{array}{l} \gamma_{11} \frac{\pi n}{R^2 + \pi^4 n^4} (\pi^2 n^2 - e^\lambda (R \sin \lambda + \pi^2 n^2 \cos \lambda) \cos \pi n) + \\ + \gamma_{12} \frac{\pi n}{R^2 + \pi^4 n^4} (R + e^\lambda (\pi^2 n^2 \sin \lambda - R \cos \lambda) \cos \pi n) + \\ + \gamma_{21} \frac{\pi n}{R^2 + \pi^4 n^4} (\pi^2 n^2 + e^{-\lambda} (R \sin \lambda - \pi^2 n^2 \cos \lambda) \cos \pi n) + \\ + \gamma_{22} \frac{\pi n}{R^2 + \pi^4 n^4} (R - e^{-\lambda} (\pi^2 n^2 \sin \lambda + R \cos \lambda) \cos \pi n) \end{array} \right).$$

Appendix III

$$\begin{aligned} \Pi_1(y) : = & \gamma_{11}^2 \Psi_1 + \gamma_{12}^2 \Psi_2 - \gamma_{11} \gamma_{12} \Psi_3 + \gamma_{21}^2 \Psi_4 + \gamma_{22}^2 \Psi_5 + \gamma_{21} \gamma_{22} \Psi_6 + \\ & + 2\gamma_{11} \gamma_{21} \Psi_7 + (\gamma_{11} \gamma_{22} - \gamma_{12} \gamma_{21}) \Psi_8 - 2\gamma_{12} \gamma_{22} \Psi_9 + \\ & + \frac{1}{2} y^2 (\gamma_{11} \gamma_{21} - \gamma_{12} \gamma_{22}), \end{aligned}$$

$$\begin{aligned} \Pi_2(y) : = & \gamma_{12}^2 \Psi_1 + \gamma_{11}^2 \Psi_2 + \gamma_{12} \gamma_{11} \Psi_3 + \gamma_{22}^2 \Psi_4 + \gamma_{21}^2 \Psi_5 - \gamma_{22} \gamma_{21} \Psi_6 + \\ & + 2\gamma_{12} \gamma_{22} \Psi_7 + (\gamma_{11} \gamma_{22} - \gamma_{12} \gamma_{21}) \Psi_8 - 2\gamma_{11} \gamma_{21} \Psi_9 - \\ & - \frac{1}{2} y^2 (\gamma_{11} \gamma_{21} - \gamma_{12} \gamma_{22}), \end{aligned}$$

$$\begin{aligned} \Pi_3(y) : = & \frac{1}{2} (\gamma_{11}^2 - \gamma_{12}^2) \Psi_3 + \frac{1}{2} (\gamma_{22}^2 - \gamma_{21}^2) \Psi_6 + \gamma_{11} \gamma_{12} \Psi_{10} + \\ & + \gamma_{21} \gamma_{22} \Psi_{11} + (\gamma_{11} \gamma_{22} + \gamma_{12} \gamma_{21}) y, \end{aligned}$$

$$\begin{aligned}
\Psi_1 &:= \frac{e^{\sqrt{2R}y} (2 + \sin \sqrt{2R}y)}{8R}, & \Psi_2 &:= \frac{e^{\sqrt{2R}y} (2 - \sin \sqrt{2R}y)}{8R}, & \Psi_3 &:= -\frac{e^{\sqrt{2R}y} \cos \sqrt{2R}y}{4R}, \\
\Psi_4 &:= \frac{e^{-\sqrt{2R}y} (2 - \sin \sqrt{2R}y)}{8R}, & \Psi_5 &:= \frac{e^{-\sqrt{2R}y} (2 + \sin \sqrt{2R}y)}{8R}, & \Psi_6 &:= \frac{e^{-\sqrt{2R}y} \cos \sqrt{2R}y}{4R}, \\
\Psi_7 &:= -\frac{\cos \sqrt{2R}y}{4R}, & \Psi_8 &:= -\frac{\sin \sqrt{2R}y}{2R}, & \Psi_9 &:= \frac{\cos \sqrt{2R}y}{4R}, \\
\Psi_{10} &:= \frac{e^{\sqrt{2R}y} \sin \sqrt{2R}y}{4R}, & \Psi_{11} &:= -\frac{e^{-\sqrt{2R}y} \sin \sqrt{2R}y}{4R}.
\end{aligned}$$

Appendix IV

$$U(k) := \begin{pmatrix} \gamma_{11}^2 q_1(k) + \gamma_{12}^2 q_2(k) - \gamma_{11} \gamma_{12} q_3(k) + \\ + \gamma_{21}^2 q_4(k) + \gamma_{22}^2 q_5(k) + \gamma_{21} \gamma_{22} q_6(k) + \\ + 2\gamma_{11} \gamma_{21} q_7(k) + (\gamma_{11} \gamma_{22} - \gamma_{12} \gamma_{21}) q_8(k) - \\ - 2\gamma_{12} \gamma_{22} q_9(k) \end{pmatrix},$$

$$V(k) := \begin{pmatrix} \gamma_{12}^2 q_1(k) + \gamma_{11}^2 q_2(k) + \gamma_{12} \gamma_{11} q_3(k) + \\ + \gamma_{21}^2 q_4(k) + \gamma_{22}^2 q_5(k) - \gamma_{22} \gamma_{21} q_6(k) + \\ + 2\gamma_{12} \gamma_{22} q_7(k) + (\gamma_{11} \gamma_{22} - \gamma_{12} \gamma_{21}) q_8(k) - \\ - 2\gamma_{11} \gamma_{21} q_9(k) \end{pmatrix},$$

$$W(k) := \begin{pmatrix} \gamma_{11} \gamma_{12} q_{10}(k) + \frac{1}{2} (\gamma_{11}^2 - \gamma_{12}^2) q_3(k) + \\ + (\gamma_{11} \gamma_{22} + \gamma_{21}^2) q_7(k) + \frac{1}{2} \gamma_{22} (\gamma_{21} - \gamma_{12}) q_8(k) + \\ + (\gamma_{12} \gamma_{21} + \gamma_{22} \gamma_{11}) q_9(k) + \gamma_{21} \gamma_{22} q_{11}(k) + \\ + \frac{1}{2} (\gamma_{22}^2 - \gamma_{21}^2) q_6(k) \end{pmatrix},$$

$$\kappa := \pi^2 (2k+1)^2,$$

$$q_1(k) = (2k+1)\pi \frac{\begin{pmatrix} \kappa^2 (\cos \sqrt{2R} + 1) + \\ + 2R\kappa (\cos \sqrt{2R} + 2 \sin \sqrt{2R}) + \\ + 8R^2 (2 + \sin \sqrt{2R}) \end{pmatrix}}{2(32R^3 + \kappa(16R^2 + 2\kappa R + \kappa^2))},$$

$$q_2(k) = (2k+1)\pi \frac{\begin{pmatrix} \kappa^2 (\cos \sqrt{2R} - 1) + \\ + 2R\kappa (2 \sin \sqrt{2R} + \cos \sqrt{2R}) + \\ + 8R^2 (\sin \sqrt{2R} - 2) \end{pmatrix}}{2(32R^3 + \kappa(16R^2 + 2\kappa R + \kappa^2))},$$

$$q_3(k) = \pi(2k+1) \frac{e^{\sqrt{2R}} \left(8R \cos \sqrt{2R} - \kappa \sin \sqrt{2R} \right) \cos \pi(2k+1) - 4R}{16R^2 + \kappa^2},$$

$$q_4(k) = (2k+1)\pi \frac{e^{-\sqrt{2R}} \left(\begin{array}{l} \kappa^2 \left(1 + \cos \sqrt{2R} \right) + \\ + 8R^2 \left(2 - \sin \sqrt{2R} \right) - \\ - 2R\kappa \left(2 \sin \sqrt{2R} - \cos \sqrt{2R} \right) \end{array} \right) + 2(8R^2 + R\kappa + \kappa^2)}{2 \left(32R^3 + 16R^2\kappa + 2R\kappa^2 + \pi^6 (2k+1)^6 \right)},$$

$$q_5(k) = (2k+1)\pi \frac{e^{-\sqrt{2R}} \left(\begin{array}{l} \kappa^2 \left(1 - \cos \sqrt{2R} \right) + 8R^2 \left(2 + \sin \sqrt{2R} \right) + \\ + 2R\kappa \left(2 \sin \sqrt{2R} - \cos \sqrt{2R} \right) \end{array} \right) + 2R(8R - \kappa)}{2 \left(32R^3 + 16R^2\kappa + 2R\kappa^2 + \pi^6 (2k+1)^6 \right)},$$

$$q_6(k) = 2\pi(2k+1) \frac{e^{-\sqrt{2R}} \left(\kappa \sin \sqrt{2R} + 4R \cos \sqrt{2R} \right) + 2R}{16R^2 + \kappa^2},$$

$$q_7(k) = \frac{- \left(2R + \kappa \left(\cos \sqrt{2R} + 1 \right) \right) - 2(R - \kappa)}{2\pi(2k+1) (\kappa - 2R)},$$

$$q_8(k) = - \frac{\left(\sqrt{2R} \left(1 - \sqrt{2R} \right) + 2\pi(2k+1) \right) \sin \sqrt{2R}}{4R - 2\kappa},$$

$$q_9(k) = - \frac{4R + \kappa \left(\cos \sqrt{2R} - 1 \right)}{2\pi(2k+1) (\kappa - 2R)},$$

$$q_{10}(k) = (2k+1)\pi \frac{\kappa \left(1 + e^{\sqrt{2R}} \cos \sqrt{2R} \right) + 4Re^{\sqrt{2R}} \sin \sqrt{2R}}{16R^2 + \kappa^2},$$

$$q_{11}(k) = (2k+1)\pi \frac{\kappa \left(1 + e^{-\sqrt{2R}} \cos \sqrt{2R} \right) - 4Re^{-\sqrt{2R}} \sin \sqrt{2R}}{(16R^2 + \kappa^2)}.$$

Appendix V

$$\begin{aligned} \Theta_1 &= \gamma_{11}^2 T_1 + \gamma_{12}^2 T_2 - \gamma_{11}\gamma_{12} T_3 + \gamma_{21}^2 T_4 + \gamma_{22}^2 T_5 + \gamma_{21}\gamma_{22} T_6 + \\ &\quad + 2\gamma_{11}\gamma_{21} T_7 + (\gamma_{11}\gamma_{22} - \gamma_{12}\gamma_{21}) T_8 - 2\gamma_{12}\gamma_{22} T_9, \\ \Theta_2 &= \gamma_{12}^2 T_1 + \gamma_{11}^2 T_2 + \gamma_{12}\gamma_{11} T_3 + \gamma_{22}^2 T_4 + \gamma_{21}^2 T_5 - \gamma_{22}\gamma_{21} T_6 + \\ &\quad + 2\gamma_{12}\gamma_{22} T_7 + (\gamma_{11}\gamma_{22} - \gamma_{12}\gamma_{21}) T_8 - 2\gamma_{11}\gamma_{21} T_9, \\ \Theta_3 &= \frac{1}{2} (\gamma_{11}^2 - \gamma_{12}^2) T_3 + \frac{1}{2} (\gamma_{22}^2 - \gamma_{21}^2) T_6 + \gamma_{11}\gamma_{12} T_{10} + \gamma_{21}\gamma_{22} T_{11} + \gamma_{11}\gamma_{22} + \gamma_{12}\gamma_{21}, \\ \Theta_4 &= \frac{\left(2R \left(R\gamma \sin 2\tau - C_0(\tau)\pi^2 (2k)^2 \right) + R \left(\pi^2 (2k)^2 K(\tau) + 8\Gamma_2 R \cos 2\tau \right) \right) \cos 2k\pi}{4k\pi \left(4R^2 + \pi^4 (2k)^4 \right)}, \end{aligned}$$

$$\begin{aligned}
T_1 &= \frac{2M_3 + M_1 + M_2}{4\sqrt{2R}}, & T_2 &= \frac{2M_3 - M_1 - M_2}{4\sqrt{2R}}, & T_3 &= \frac{M_2 - M_1}{2\sqrt{2R}}, \\
T_4 &= \frac{M_5 - M_4 - 2M_9}{4\sqrt{2R}}, & T_5 &= \frac{M_4 - M_5 - 2M_9}{4\sqrt{2R}}, & T_6 &= -\frac{M_4 + M_5}{2\sqrt{2R}}, \\
T_7 &= \frac{1}{2}M_6 + \frac{1}{2\sqrt{2R}}M_7, & T_8 &= -\frac{M_8}{\sqrt{2R}}, & T_9 &= -\frac{M_7}{2\sqrt{2R}} + \frac{1}{2}M_6, \\
T_{10} &= \frac{M_1 + M_2}{2\sqrt{2R}}, & T_{11} &= \frac{M_5 - M_4}{2\sqrt{2R}},
\end{aligned}$$

$$M_1 = -k\pi \frac{\pi^2 k^2 \left(e^{\sqrt{2R}} \cos \sqrt{2R} - 1 \right) + R e^{\sqrt{2R}} \sin \sqrt{2R}}{2(R^2 + \pi^4 k^4)},$$

$$M_2 = -k\pi \frac{R \left(1 - e^{\sqrt{2R}} \cos \sqrt{2R} \right) + \pi^2 k^2 e^{\sqrt{2R}} \sin \sqrt{2R}}{2(R^2 + \pi^4 k^4)},$$

$$M_3 = \frac{e^{\sqrt{2R}} \left(\sqrt{2R} \sin 2k\pi - 2k\pi \right) + 2k\pi}{4\pi^2 k^2 + 2R},$$

$$M_4 = \frac{\pi^2 k^2 \left(1 - 16\pi^3 k^3 e^{-\sqrt{2R}} \cos \sqrt{2R} \right) + R e^{-\sqrt{2R}} \sin \sqrt{2R}}{4(R^2 + \pi^4 k^4)},$$

$$M_5 = -k\pi \frac{\pi^2 k^2 e^{-\sqrt{2R}} \sin \sqrt{2R} + R \left(e^{-\sqrt{2R}} \cos \sqrt{2R} - 1 \right)}{2(R^2 + \pi^4 k^4)},$$

$$M_6 = -\frac{1}{2k\pi}, \quad M_7 = \frac{k\pi \sin \sqrt{2R}}{R - 2\pi^2 k^2}, \quad M_8 = \frac{k\pi \left(\cos \sqrt{2R} - 1 \right)}{R - 2\pi^2 k^2}, \quad M_9 = \frac{k\pi \left(1 - e^{-\sqrt{2R}} \right)}{R + 2\pi^2 k^2}.$$

Received for publication 21 January 2015